# Research Interest

Niladri Gomes

May 4, 2017

## 1 Motivation

Determination of the mechanism of superconductivity (SC) in correlated electron superconductors is one of the most challenging problems in condensed matter physics. Recent discovery of an ubiquitous charge ordered (CO) state proximate to (SC) within the pseudo-gap phase of cuprates [10, 11, 12, 14] has given the problem a new complexity. A quantum critical transition that separates the under-doped and over-doped copper oxides has been proposed as well as debated [2, 21, 33]. It is highly relevant in this context that there exist other correlated-electron superconductors where also quantum criticality plays a crucial role; where SC is proximate to CO (with sometimes anitiferromagnet (AFM) a neighboring phase), but is reached not by doping but by application of pressure that modifies the one-electron bandwidth. It is conceivable that the determining the mechanism of correlated-electron SC in these "cleaner" systems is simpler, and that they may provide fresh insight to the problem as a whole. With this motivation my research interests have been mostly to investigating on the mechanism and relationships between various broken symmetry phases, magnetism and SC in organic charge transfer solids (CTS).

## 2 Overview of organic CTS

CTS are hole carriers $A_2X$, where A is an organic molecule (TMTSF, BEDT-TTF, BETS, etc.) and X is an inorganic monovalent closed-shell anion ($PF_6$, $ClO_4$, $Cu(NCN)_2Cl$, $Cu(NCS)_2$, etc.); or electron-carriers $Z[Pd(dmit)_2]_2$, where Z is a closed-shell monovalent cation. In all cases electronically active 2D organic layers are separated by inactive inorganic layers. In my research I have focussed on hole carriers $(BEDT\text{-}TTF)_2X$. Depending on the anion, $(BEDT\text{-}TTF)_2X$ have different crystal structures, which are referred to as $\alpha$, $\beta$, $\kappa$, $\theta$ etc. The common features shared by all superconducting CTS are quasi-two-dimensionality of the active organic layers, strong e-e repulsion, geometric lattice frustration and carrier density ($\rho$= 0.5) ($\rho$ = No of carriers/No of sites) per molecule.

### 2.1 Broken symmetries and SC

The superconducting states in the CTS are often proximate to AFM, quantum spin liquid (QSL) or CO. Pressure-induced AFM-to-SC in $\kappa$-$(BEDT\text{-}TTF)_2X$, with X = $Cu(NCN)_2Cl$ and deuterated $Cu(NCN)_2Br$, and QSL-to-SC in X = $Cu_2(CN)_3$ have led to speculations that spin fluctuations are responsible for the SC [20, 28, 35]. However, CO-to-SC transitions are also common and are seen in the $\alpha$, $\theta$, $\beta$ and $\beta''$-(BEDT-TTF) compounds, as well as in the electron carrier $EtMe_3P[Pd(dmit)_2]_2$.

$\kappa$-$(BEDT\text{-}TTF)_2$ are strongly dimerized, with the intradimer hopping integrals significantly larger than the interdimer hoppings. The dimer unit cell contains 1 hole on the average, which has led to effective 1/2-filled band Hubbard [100–108] and Hubbard- Heisenberg U-$t$-$J$ [65–67, 116–118] models for $\kappa$-$(BEDT\text{-}TTF)_2X$. The dimer lattice is anisotropic triangular, and for weak anisotropy the effective model successfully explains the experimentally observed AFM[119, 120]. Precise numerical work by our group [6, 9, 16] and others [41, 43] have however shown that there is no superconducting order within the $\rho = 1$ triangular lattice Hubbard band for any anisotropy and U. Pair correlations are enhanced by U only for nearest-neighbor pairs, but this reflects AFM spin coupling and not SC.

### 2.2 Effective e-e attraction and spin singlet states in $\rho$ =0.5

It has often been surmised that correlated electron SC evolves upon doping a spin-gapped semiconductor, as would occur in toy models such as a 2D lattice consisting of weakly coupled even-leg ladders [3, 42].

Finding realistic 2D models with spin gap (SG) and enhanced pair correlations however has remained challenging. A bond charge modulated spin-Peierls state is seen in quasi-1D $\rho = 0.5$ CTS called Paired Electron Crystal (PEC) [7]. Similar PECs occur in the $\rho = 0.5$ zigzag ladder [5] and in the 2D anisotropic triangular lattice for sufficiently large lattice frustration [8, 22]. Our idea is destabilization of the PEC, either by weak doping, or due to increase of frustration (which could be a pressure-induced effect in real CTS) would lead to pair tunneling, giving rise to a paired-electron liquid (PEL) with superconducting pair correlations. In the next section results of our recent numerical calculations [17] are presented, which is a numerical demonstration of enhanced SC pair correlation at $\rho \approx 0.5$.

## 2.3 Numerical demonstration of enhanced SC pair correlation at $\rho \approx 0.5$.

The standard singlet pair-creation operator is defined as

$$\Delta_i^\dagger = \frac{1}{\sqrt{2}} \sum_{\vec{\nu}} g(\vec{\nu})(c_{i,\uparrow}^\dagger c_{i+\vec{\nu},\downarrow}^\dagger - c_{i,\downarrow}^\dagger c_{i+\vec{\nu},\uparrow}^\dagger). \tag{1}$$

The phases $g(\vec{\nu})$ determine the symmetry of the superconducting pairs. In our calculations we considered $s$, $d_{x^2-y^2}$, and $d_{xy}$ pairing symmetries.We calculated [17] the equal-time pair-pair correlations $P_{ij} = \langle \Delta_i^\dagger \Delta_j \rangle$,for four different periodic anisotropic triangular lattices, 4×4, 6×6, 10×6 and 10×10, with the widest possible carrier densities $0 < \rho < 1$, using four different numerical techniques. The complete

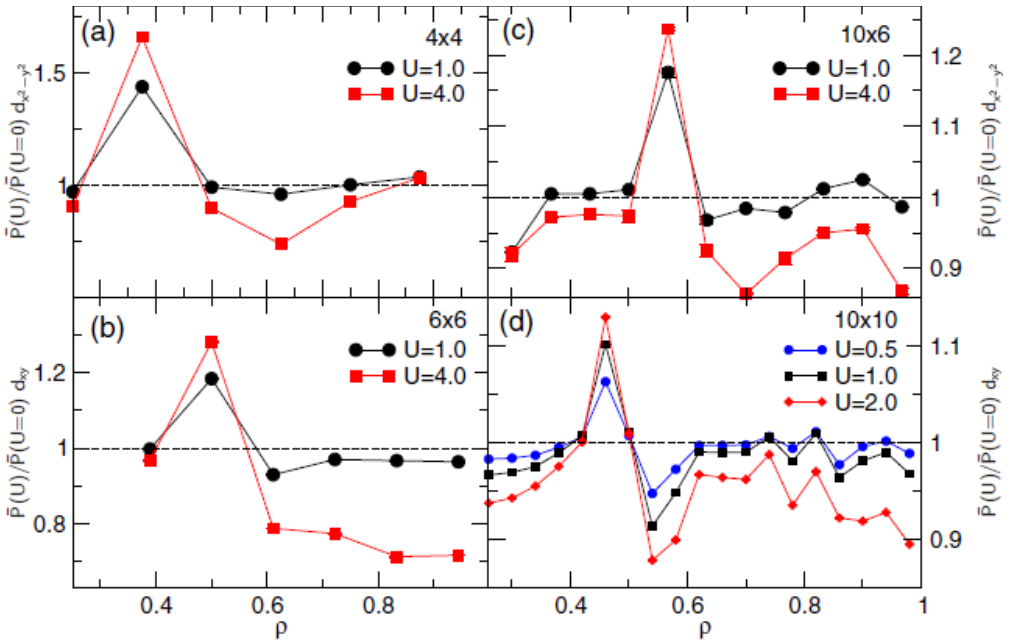


Figure 1: (color online) Average long range pair-pair correlation $\bar{P}(U)$ normalized by its uncorrelated value for (a) 4×4, (b) 6×6, (c) 10×6 and (d) 10×10 anisotropic triangular lattices, for $t_y = 0.9$ and $t_{x+y} = 0.8$. 4×4 results are exact; 6×6 and 10×6 results are obtained using the Path Integral Renormalization Group (PIRG) method; and 10×10 by the Constrained Path Monte Carlo (CPMC) method.

results, summarized in Fig. 1, are remarkable: Coulomb interactions enhance superconducting pair correlations only in a narrow density range close to $\rho = 0.5$. For each lattice $\bar{P}(U)/\bar{P}(U = 0) > 1$ for a single $\rho$ that is either exactly 0.5 or one of two closest carrier fillings with closed shell Fermi level occupancy at $U = 0$. Pair correlations are suppressed by $U$ at all other $\rho$, including the region $0.7 < \rho < 1$ that has been extensively investigated in the context of cuprate SC [33]. In three of four lattices in Fig. 1 enhancement of $\bar{P}(U)$ occurs for $\rho$ slightly away from 0.5. Importantly, the deviation from 0.5 of the $\rho$ at which $\bar{P}(U)$ is enhanced (excluding the 6×6 lattice where this deviation is zero) decreases monotonically with size.

In a different calculation on the monomer lattices of the organic charge-transfer solids $\kappa$-(BEDT-TTF)$_2$X, for 32 and 64 molecular sites, we found that d-wave superconducting pair-pair correlations are enhanced by electron-electron interactions only for a narrow carrier concentration about $\rho = 0.5$ [37].

The numerical ground state results have been further confirmed by finite temperature Determinantal Quantum Monte Carlo (DQMC) calculations.

# 3 Methods

Computational methods were an important part of our work. Here I briefly summarize the methods we adopted to carry out the research.

## 3.1 Valence Bond (VB) diagonalization

The VB method used spin adapted VB diagram basis for studying correlated quantum systems [31, 38, 44]. The advantage of VB methodover methods conserving only $S_z$ are that it allows visualization of wavefunctions in terms of dominant VB diagrams.

## 3.2 Determinantal Quantum Monte Carlo (DQMC)

DQMC allows simulation of Hubbard-type models by integrating out the fermion degrees of freedom, replacing the Hubbard interaction with an auxilliary Hubbard-Stratonovich field [4, 24]. The method suffers from sign problem when used for fermion systems. Electron phonon-coupling can also be treated within DQMC [19].

## 3.3 Path Integral Renormalization Group (PIRG)

In the PIRG method, the wavefunction is expanded as a sum over $L$ Slater determinants, and the projector operator $\exp(-\tau H)$ is used to project out the ground state from a random starting determinant [39]. The method is exact at $U = 0$ and for each $L$ PIRG calculations are variational. The finite bias is removed by extrapolating quantities as a function of the energy variance $\Delta E$. Importantly, PIRG doesn't suffer from sign problem.

Several additional techniques are essential to improve the accuracy of the PIRG. The use of lattice and spin symmetries using projection operators of the QP-PIRG has been shown to drastically lower the energy [40].Second, it has been observed that PIRG method can get stuck in excited states. To prevent this, in addition to the PIRG projection operator, we used a random simulated annealing-like modification of the Slater determinants [32]. Furthermore, several starting states were chosen and theri final energy were compared.

We have extensively benchmarked against the exact VB method and have found essentially prefect agreement [8]. The main disadvantage of PIRG compared to DQMC and CPMC is that it is much more computationally expnsive.

## 3.4 Constrained Path Monte Carlo (CPMC)

CPMC is a ground-state projector QMC method [45].Like PIRG, CPMC works in the space of Slater determinants. This space is overcomplete, which results in contributions to the ground state wavefunction that are both positive and negative. The Monte Carlo sampling is confined to the region where the overlap between each random walker $|\phi\rangle$ and a trial wavefunction $|\Psi_T\rangle$ is positive. This eliminates the loss of precision known as the fermion sign problem, but introduces an approximation into the method. A recent advance is the use of symmetry-adapted trial wavefunctions with CPMC, which greatly improves the accuracy [36]. We have used symmetry-adapted trial functions. The PIRG wavefunctions are ideal for this use.

# 4 Future Directions

While the pairing enhancement at a specific carrier density is intriguing and can have far reaching implications, our results miss two important aspects. First, in our calculation for the different lattices,

the enhancement occurs in either the $d_{x^2-y^2}$ or $d_{xy}$ channels, that is the pairing symmetry varies. Second, even as the density $\rho$ where enhancement occurs tends to $\rho \approx 0.5$ as the lattice size increases, the precise $\rho$ where the enhancement occurs is different on each lattice. The evolving phase diagram and continuous dicovery of exotic phenomena in the unconventional superconductors has kept the field vibrant. The future scope of research thus, is many-fold. The CO state is known to be accompanied by giant phonon anomalies [23]. The effect of phonon could be studied as a combined effect of e-e and e-ph interactions in 2D systems within the Hubbard -Holstein model. Prior numerical calculations have been limited to $\rho = 1$ [19, 30]. Hubbard-Holstein model in 1D has been extensively studied using Stochastic Series Expansion (SSE) QMC [5, 18]. To add the effect of phonons, the variation of position coordinate of each oscillator will require an additional Monte Carlo sampling. The bare Hubbard model is sign-free at $\rho = 1$. Addition of e-ph interaction to the model has shown sign problem in the square lattice $\rho = 1$ limit [19]. Code development for the Hubbard-Holstein model to study pairing correlation and bond coupled e-ph model may be of interest.

Finally, aside from their application in strong correlation physics, numerical methods are heavily used in a wide range of multiscale problems. The ab-initio molecular dynamics (MD), density functional theory (DFT), biophysics of protein folding [29, 34], multiscale optical design [27] are to name a few. The fluidity of applicability of algorithms and numerical techniques have been exploited by computational physicists in MD simulations[25, 26], transport across cellular membranes [1, 13], modeling of cell motion and shape using elasticity theory[15]. The dynamic and interdisciplinary nature of numerical methods is what excites me the most. In future I would like to dive deeper into learning different algorithms and their implementations and explore more the "fluidity" of the field.

# References


[1] J.L. Adelman, C. Ghezzi, P. Bisignano, D.D.F. Loo, S. Choe, J. Abramson, J.M. Rosenberg, E.M. Wright, and M. Grabe. *Proc. Natl. Acad. Sci. USA*, 113:E3960–E3966, 2006.

[2] P. W. Anderson, P. A. Lee, M. Randeria, T. M. Rice, N. Trivedi, and F. C. Zhang. *J. Phys.: Condens. Matter*, 16:R755, 2004.

[3] E. Arrigoni, E. Fradkin, and S. A. Kivelson. *Phys. Rev. B*, 69:214519, 2004.

[4] R. Blankenbecler, D. J. Scalapino, and R. L. Sugar. *Phys. Rev. D*, 24:2278, 1981.

[5] R. T. Clay and S. Mazumdar. *Phys. Rev. Lett.*, 94:207206, 2005.

[6] R. T. Clay, H. Li, and S. Mazumdar. *Phys. Rev. Lett.*, 101:166403, 2008.

[7] R. T. Clay, J. P. Song, S. Dayal, and S. Mazumdar. *Phys. Rev. Lett.*, 101:166403, 2012.

[8] S. Dayal, R.T.Clay, H.Li, and S.Mazumdar. *Phys. Rev. B*, 83:245106, 2011.

[9] S. Dayal, R. T. Clay, and S. Mazumdar. *Phys. Rev. Lett.*, 85:165141, 2012.

[10] G. Ghiringhelli et al. *Science*, 337:821, 2012.

[11] J. Chang et al. *Nature Physics*, 8:871, 2012.

[12] R. Comin et al. *Science*, 343:390, 2014.

[13] S Veshaguri et. al. *Science*, 351:1469, 2016.

[14] T. Wu et al. *Nat. Commun.*, 4:2113, 2013.

[15] Raymond E. Goldstein, Alain Goriely, Greg Huber, and Charles W. Wolgemuth. *Phys. Rev. Lett.*, 84:1631, 2000.

[16] N. Gomes, R. T. Clay, and S. Mazumdar. *J. Phys.: Condens. Matter*, 25:385603, 2012.

[17] N. Gomes, W. De Silva, R. T. Clay, and S. Mazumdar. *Phys. Rev. B*, 93:165110, 2016.

[18] R. P. Hardikar and R. T. Clay. *Phys. Rev. B*, 75:245103, 2007.

[19] S. Johnston, E. A. Nowadnick, B. Moritz Y. F. Kung, R. T. Scalettar, and T. P. Devereaux. *Phys. Rev. B*, 87:235133, 2013.

[20] H. Kino and H. Kontani. *J. Phys. Soc. Jpn.*, 67:3691, 1998.

[21] P. A. Lee, N. Nagaosa, and X. G. Wen. *Rev. Mod. Phys.*, 78:17, 2006.

[22] H. Li, R. T. Clay, and S.Mazumdar. *J. Phys.: Condens. Matter*, 22:272201, 2010.

[23] Ye-Hua Liu, Robert M. Konik, T.M. Rice, and Fu-Chun Zhang. *Nat. Commun.*, 7:10378, 2015.

[24] E. Y. Loh and J. E. Gubernatis. *Elsevier*, pages 177–235, 1992.

[25] D. Marx and M. Parrinello. *J. Chem. Phys.*, 58:57, 1996.

[26] Guglielmo Mazzola and Sandro Sorella. *Annu. Rev. Phys. Chem.*, 58:57, 2007.

[27] Predrag Milojkovic and Marc P. Christensen. *Applied optics*, 54:171, 2015.

[28] A. H. Nevidomskyy, C. Scheiber, D. Sénechal, and A.-M. S. Tremblay. *Phys. Rev. B*, 77:064427, 2008.

[29] B. Nolting. *Protein Folding Kinetics: Biophysical Methods (Springer, New York,)*, 2005.

[30] E. A. Nowadnick, S. Johnston, B. Moritz, R. T. Scalettar, and T. P. Devereaux. *Phys. Rev. Lett.*, 109:246404, 2012.

[31] S. Ramasesha and Z. G. Soos. *Int. J. Quant. Chem.*, XXV:1003, 1984.

[32] P. Sahebsara and D. Sénéchal. *Phys. Rev. Lett.*, 97:257004, 2006.

[33] D. J. Scalapino. *Rev. Mod. Phys.*, 84:1383, 2012.

[34] H. A. Scheraga, M. Khalili, and A. Liw. *Annu. Rev. Phys. Chem.*, 58:57, 2007.

[35] J. Schmalian. *Phys. Rev. Lett.*, 81:4232, 1998.

[36] H. Shi, C. A. Jimenez-Hoyos, R. Rodriguez-Guzman, G. E. Scuseria, and S. Zhang. *Phys. Rev. B*, 89:125129, 2014.

[37] W. De Silva, N. Gomes, S. Mazumdar, and R. T. Clay. *Phys. Rev. B*, 93:205111, 2016.

[38] Z. G. Soos and S. Ramasesha. *Phys. Rev. B*, 29:5410, 1984.

[39] Kashima T and Imada M. *J. Phys. Soc. Jpn.*, 70:2287–99, 2001.

[40] T.Mizusaki and M.Imada. *Phys. Rev. B*, 74:014421, 2006.

[41] L. F. Tocchio, A. Parola, C. Gros, and F. Becca. *Phys. Rev. B*, 80:064419, 2009.

[42] Matthias Troyer, Hirokazu Tsunetsugu, and T. M. Rice. *Phys. Rev. B*, 53:251, 1996.

[43] T. Yanagisawa. *New J. Phys*, 15:033012, 2013.

[44] S. Zhang, J. Carlson, and J. E. Gubernatis. *Chem. Phys. Lett*, 130:522, 1986.

[45] S. Zhang, J. Carlson, and J. E. Gubernatis. *Phys. Rev. B*, 69:7464, 1997.